PHYSICAL REVIEW B VOLUME 42, NUMBER 4 1 AUGUST 1990

Thermodynamics and phase diagram of multilayer krypton on graphite

R. Gangwar and R. M. Suter
Department of Physics, Carnegie-Mellon University, Pittsburgh, Pennsylvania 15213
(Received 2 April 1990)

We have studied the growth of the first three layers of krypton on graphite using high-resolution vapor-pressure isotherms at temperatures near the low-temperature layering critical points. Well below the critical temperatures the isotherms are consistent with a simple stacking of ordered hexagonal layers. At higher temperatures, there is a two-transition sequence in the second layer with a condensation transition followed by a weak anomaly which probably indicates breaking of the symmetry associated with the two degenerate ways of stacking hexagonal layers. This weak transition persists above the second-layer critical point. We analyze the isotherm shapes and find that the critical behavior weakens appreciably with layer number. Even at two layers, the critical behavior appears to deviate from the two-dimensional Ising model.

Recent work has demonstrated that the physics of multilayer physisorbed films is surprisingly rich. A new class of first-order phase transitions has been discovered,[1,2] evidence of surface melting[3,4] and surface roughening[4] has been seen, and structural mismatch between layers has been reported.[5] In fact, the simple theoretical picture of the phase diagram of a solid wetting film[6] containing a sequence of layering critical points which extrapolate to the bulk surface roughening temperature appears to be a considerable oversimplification.[7] It is clear that both in-plane disorder and vertical fluctuations are important even in films only a few layers thick.[3,5,8] What is needed at this point is a microscopic picture of how a several-layer-ordered film grows: What are the structures and phase transitions, how and when do vertical fluctuations manifest themselves, and how do these fluctuations play a role in melting transitions? These are important questions because the nature of the first few layers is crucial in determining the extent of wetting of a solid substrate by an ordered film.

In this Rapid Communication, we present a study of (1-3)-layer-thick krypton films on graphite. Thermodynamic data based on high-precision vapor-pressure isotherms yield previously unobserved features in the phase diagram and allow an analysis of fluctuation phenomena near the layering critical points. Much of the recent work on the krypton on graphite system is summarized by Specht *et al.*[9] The region of the phase diagram of interest here has been studied recently by Hess' group[2,10] and by Larher's group.[11,12] Our results are consistent with previous work but represent a significant extension.

The sample and apparatus used here have been described elsewhere.[13,14] We measure the coverage as a function of chemical potential μ obtained from pressure and temperature measurements and the ideal gas form of μ. The coverage Θ is normalized to fully incommensurate monolayer units. This amount is 10% more than the commensurate $\sqrt{3}\times\sqrt{3}$ amount. We compute the susceptibility $\chi=\delta\Theta/\delta\mu$ by taking coverage and chemical-potential differences between neighboring isotherm data points without numerical smoothing. χ is a particularly convenient quantity since in a first-order coexistence region it diverges and near a condensation critical point it is analogous to the Ising-model magnetic susceptibility (see below).

Figure 1 shows χ plotted against μ. At the lowest temperatures, we observe peaks in χ which are roughly 0.5 K wide in μ in the second layer and even less in the third. At $T=92.47$ K, these peaks correspond to deposition of 0.7 ML (ML denotes monolayer). Obviously, these are the first-order layering transitions. These transitions are the sharpest ones we have observed on exfoliated graphite.[15-17] We conclude from the low-temperature data

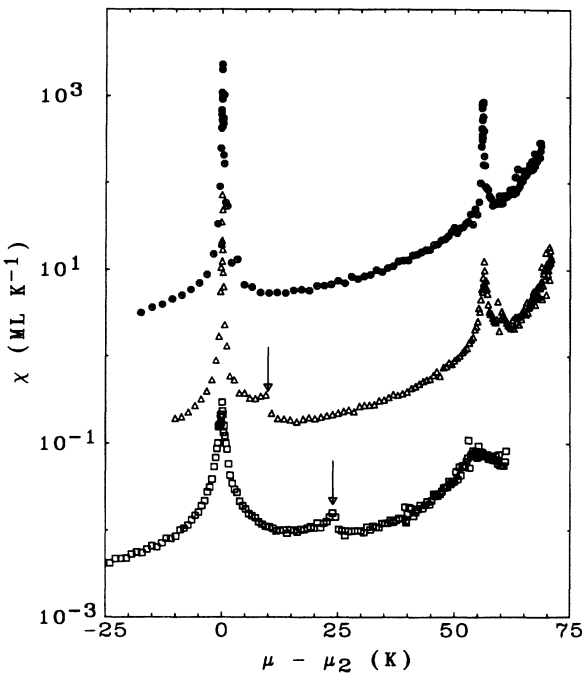

FIG. 1. The susceptibility in the second- and third-layer region. Note the logarithmic scale: χ varies by as much as four decades in a given run. Circles are data collected at 92.47 K, triangles at 96.46 K, and squares at 99.76 K; the data sets have been multiplied by 1000, 30, and 1, respectively. The arrows indicate the weak anomaly in the second layer.

 ©1990 The American Physical Society

that several-layer-thick noble-gas films on *ZYX* graphite are extremely clean thermodynamic systems which warrant quantitative study.

In the high-temperature limit of the data, we observe a continuous behavior in χ indicating that we have passed the critical points which terminate the first-order layering transitions at T_{c2} and T_{c3}. In Fig. 1 the run at $T=99.76$ K is above T_{c2} and T_{c3} whereas the run at $T=96.46$ K is above T_{c3} but not T_{c2}. Evidently, $T_{c2} > T_{c3}$.

In addition to the two layering peaks, two of the data sets shown also contain a small anomaly between the two condensation peaks. This barely measurable peak appears consistently in isotherms taken at temperatures above 93 K. This anomaly appears below T_{c2} and persists to the highest temperature at which we have done measurements.

Figure 2 shows the chemical-potential–temperature phase diagram deduced from our coverage data; not shown are the layering lines which lie between the third-layer transition and the bulk solid.[16] The layer critical temperatures deduced from detailed analysis discussed below are $T_{c2}=98.2(3)$ K and $T_{c3}=96.2(3)$ K; these values are consistent with the work of others.[2,11] The weak anomalies in the second-layer separate from the condensation line at $T\simeq 93$ K. Because of the weakness of the signal, we do not speculate on the order of this transition.

We now discuss what is probably the simplest physical scenario consistent with Fig. 2. The description is based on the stacking of ordered hexagonal layers needed to grow a bulk crystal. (i) The first layer occupies *A* sites (the monolayer is expected to be incommensurate with the substrate; we therefore ignore substrate effects). (ii) For the second layer, the energies on *B* and *C* sites are equal. To form a commensurate (with the first layer) second layer, this site symmetry must be broken. (iii) A third-layer atom or cluster of atoms on top of an *A-B* ordered bilayer will prefer to occupy either *A* or *C* sites because of the difference in interactions with the first layer. Thus, there is, in principle, no further symmetry breaking after the second layer. This scenario is consistent with Saam's "fcc model" phase diagram.[18]

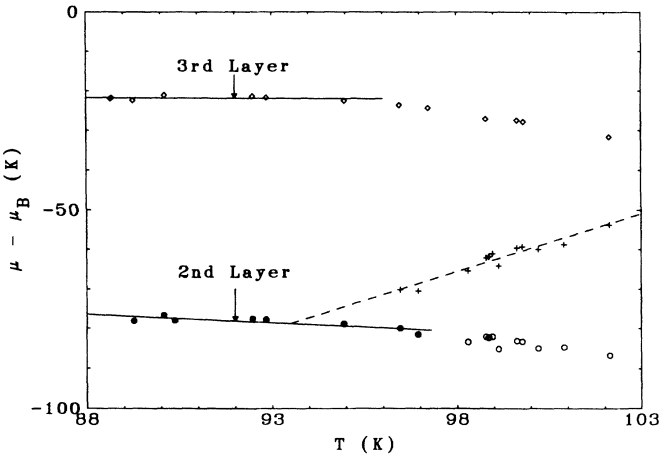

FIG. 2. The chemical-potential–temperature phase diagram of multilayer krypton on graphite. The chemical-potential scale shows the difference from the bulk solid condensation value, $\mu_B(T)$. Symbols represent the positions of maxima in χ. Solid lines are first-order transitions including second- and third-layer condensation. The dashed line is the locus of "weak" anomalies near $\Theta=2$ ML; we do not speculate on the order of this transition. Data points above the critical points do not represent phase transitions but only nonsingular maxima in χ.

The above scenario leads to the following interpretation of Fig. 2. In the second layer at low temperatures the layering line indicates coexistence between a dilute second-layer vapor and a dense and fully ordered bilayer phase. As the temperature increases towards T_{c2}, the coexistence region narrows and disorder is permitted in the dense phase; the transition is now liquid-gas-like rather than sublimation-like. Increasing μ above the dashed line in Fig. 2 leads to the symmetry-breaking transition which must enclose the ordered bilayer. The third layering line is a lattice-gas condensation transition on a single sublattice. A similar second-layer phase diagram has recently been observed for CO on graphite.[19]

Having established the phase diagram and having noted that the transition signals are strong and sharp, we turn to a detailed characterization of the data near the critical points. We use a least-squares-fitting procedure in analyzing the coverage data. Condensation transitions are expected to fall in the Ising-model universality class. The magnetization is replaced with the coverage difference from the midpoint of coexistence $\Delta\Theta$ and the magnetic field becomes the chemical-potential difference $\Delta\mu$ from the same point. While the two-dimensional Ising model is exactly solved in zero field, there is no solution for the field dependence. We use an empirically justified approach: At T_c, we expect $\Delta\Theta\sim\Delta\mu^{1/\delta}$ or $\chi\sim\Delta\mu^{-(1-1/\delta)}$. Above T_c, χ should have a finite peak and tails that approach a power law as $T\rightarrow T_c$. We suppose that

$$\chi=c\left[\left(\frac{\Delta\mu}{\mu_0}\right)^2+1\right]^{-1/2+\epsilon} . \tag{1}$$

This function has power-law tails $|\Delta\mu/\mu_0|^{-1+2\epsilon}$. As $T\rightarrow T_c$, we expect $\mu_0\rightarrow 0$, $c\sim(T-T_c)^{-\gamma}$, and $\epsilon\rightarrow 1/(2\delta)$. For the two-dimensional Ising model, $\gamma=\frac{7}{4}$ and $\delta=15$. Away from T_c, ϵ will be an effective exponent.

Our direct measurement is of Θ, rather than χ. Therefore, we fit to Θ, which contains the integral of (1) plus a regular background which we take to be quadratic:

$$\Theta=\Theta_0+a\Delta\mu+b(\Delta\mu)^2+c\int_0^{\Delta\mu}dx\left[\left(\frac{x}{\mu_0}\right)^2+1\right]^{-1/2+\epsilon} . \tag{2}$$

The integral involves incomplete beta functions in different forms when ϵ is positive and negative; details will be given in a forthcoming publication.[20] Finally, we convolve (2) (numerically) with a Gaussian smearing function in order to account for the substrate heterogeneity. From the width of low-temperature peaks in χ, we are led to choose a 0.25-K e^{-1} width for the second-layer data and a 0.1-K e^{-1} width for the third layer. The convolution has a negligible effect except for the data nearest to T_{c2} where the peak in χ is quite sharp. We perform weighted fits which adjust the parameters ϵ, μ_0, and c as

well as the background terms. While this is a large number of parameters, there are only three which describe the precritical anomaly; also, the quadratic term makes a negligible contribution for all second-layer data. Results are shown in Fig. 3. The fits are excellent: deviations appear random and, except where the slope is large (where small errors in μ generate large errors in Θ), are of the order of 10^{-3} ML. Fits to (2) fail dramatically below the assigned critical temperatures.

The amplitude c and width μ_0 are shown in Fig. 4.[21] Also, for second-layer data, ϵ has a roughly linear variation from $\simeq -0.3$ at 3 K above T_{c2} to roughly zero at 98.2 K. The fact that ϵ approaches zero is consistent with a large value of the critical exponent δ. In the third layer, ϵ is again negative and approaches zero as $T \rightarrow T_{c3}$; further details of its temperature dependence are ill-defined due to the weakness of the anomaly. There is an obvious qualitative distinction between the two layering critical points: critical behavior is much weaker near T_{c3}. For data close to T_{c2}, the parameters indicate a substantial region of $\Delta\mu$ in which power-law behavior is seen: μ_0 becomes less than 1 K and the amplitude becomes large compared to the background. On the other hand, no power-law region is accessible in the third layer. In layered liquid films it appears that the opposite trend with layer number is observed.[22]

Figure 4 shows power-law fits to c and μ_0 for the second-layer data. The fit to c, shown as the solid line in Fig. 4(a), yields $T_{c2}=98.1(2)$ K and $\gamma=1.24(8)$. The fit to $\mu_0(T)$ yields $T_{c2}=98.4(2)$ K and a positive exponent of 1.4(2). Given the variation in ϵ with temperature, it is not clear that μ_0 should necessarily follow a simple power law, but to the accuracy of the data, the fit is quite good and the value of T_{c2} is consistent with the fit to c. While the data do not yield precise exponents, we find it surprising that we consistently obtain values far from those of the two-dimensional Ising model. In addition to the power-law fits shown here, we have attempted a scaling function analysis of the data. Excellent scaling can be obtained, but the exponents are again not those of the Ising model.[20]

To summarize, we have observed a previously unobserved phase transition in the second layer of krypton on *ZYX* graphite, established the phase diagram geometry, and probed critical behavior near the second- and third-layering critical points. The phase-transition signals are surprisingly clean and heterogeneous smearing is almost negligible. Thus, the high-precision data and the physical system are well matched. The observed non-Ising behavior probably reflects a narrow asymptotic critical region. Critical behavior over the 5-K region above T_{c2} may be coupled to significant changes in layer promotion populations. We have begun x-ray scattering work to address these issues. Rotating anode data[23] are consistent with our hypotheses concerning the low-temperature phases and with the presence of disorder in the second-layer intermediate phase.

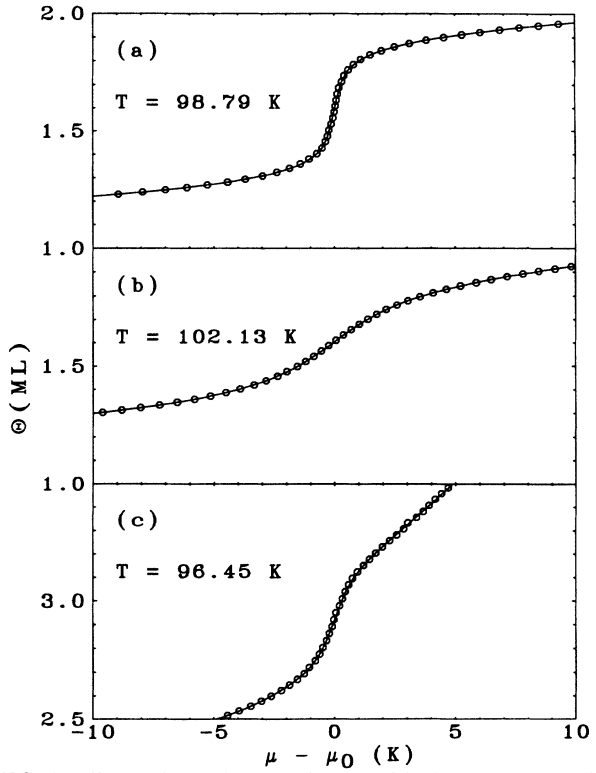

FIG. 3. Illustrations of fits to the precritical anomalies in the coverage isotherms. (a) and (b) are second-layer data while (c) is in the third layer. μ_0 is the point of maximum slope. Note that, while (c) is only 0.2 K above T_{c3}, the anomaly is small compared to that in (a) which is 0.4 K above T_{c2}. It is also evident that the background terms in Eq. (2) are more important in the third layer than in the second.

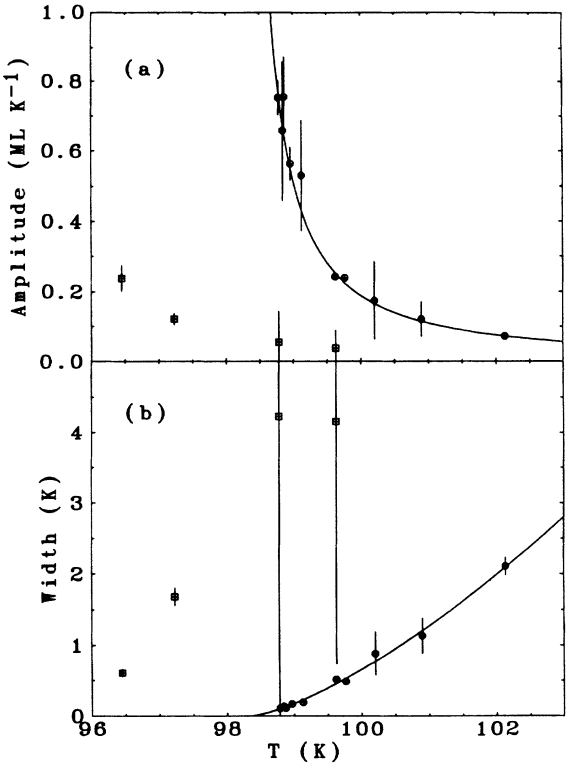

FIG. 4. Summary of the fits to second- and third-layer isotherms. Circles are second-layer data, while squares are third-layer data. Solid lines through the second-layer data are power-law fits discussed in the text. (a) shows the evolution in the peak value of χ. (b) shows the width parameter μ_0.

We have enjoyed helpful conversations with S. Garoff, R. B. Griffiths, and R. Swendsen. We thank W. Wang for helping with data collection. This work has been supported by an IBM Computer Related Materials grant.

[1]H. S. Youn and G. B. Hess, Phys. Rev. Lett. **64**, 918 (1990).
[2]H. S. Youn, D. M. Li, and G. B. Hess, Bull. Am. Phys. Soc. **35**, 592 (1990).
[3]J. Z. Larese and Q. M. Zhang, Phys. Rev. Lett. **64**, 922 (1990).
[4]D. Zhu and J. G. Dash, Phys. Rev. B **38**, 11673 (1988).
[5]J. Z. Larese, M. Harada, L. Passell, J. Krim, and S. Satija, Phys. Rev. B **37**, 4735 (1988).
[6]M. J. de Oliviera and R. B. Griffiths, Surf. Sci. **71**, 687 (1978).
[7]G. An and M. Schick, Phys. Rev. B **37**, 7534 (1988).
[8]C. D. Hruska and J. M. Phillips, Phys. Rev. B **37**, 3801 (1988); J. M. Phillips and C. D. Hruska, *ibid.* **39**, 5425 (1989).
[9]E. D. Specht *et al.*, Z. Phys. B **69**, 347 (1987).
[10]H. S. Nham and G. B. Hess, Langmuir **5**, 575 (1989).
[11]Y. Larher and F. Angerand, Europhys. Lett. **7**, 447 (1988).
[12]Y. L. F. Ser and B. Gilquin, Mol. Phys. **67**, 1077 (1989).
[13]R. M. Suter, N. J. Colella, R. Gangwar, and W. Wang, Rev. Sci. Instrum. **58**, 462 (1987).
[14]R. Gangwar, N. J. Colella, and R. M. Suter, Phys. Rev. B **31**, 627 (1989).
[15]R. E. Ecke, J. G. Dash, and R. D. Puff, Phys. Rev. B **26**, 1288 (1982).
[16]J. G. Dash and R. D. Puff, Phys. Rev. B **24**, 295 (1981).
[17]R. M. Suter, N. J. Colella, and R. Gangwar, Phys. Rev. B **31**, 627 (1985).
[18]W. F. Saam, Surf. Sci. **125**, 253 (1983).
[19]Y. P. Feng and M. H. W. Chan (unpublished).
[20]R. Gangwar and R. M. Suter (unpublished).
[21]The large error bars on the high-temperature data points in the third layer are due to the weakness of the precritical anomaly and a sparse set of data points in the third-layer region in these isotherms.
[22]H. S. Nham and G. B. Hess, Phys. Rev. B **38**, 5166 (1988).
[23]R. Hainsey and R. M. Suter (unpublished).